WPMAT-PR(18) 21280

P Jenus et al.

W2C-reinforced tungsten prepared using different precursors

Preprint of Paper to be submitted for publication in
Ceramics International

This work has been carried out within the framework of the EUROfusion Consortium and has received funding from the Euratom research and training programme 2014-2018 under grant agreement No 633053. The views and opinions expressed herein do not necessarily reflect those of the European Commission.

W_2C-reinforced tungsten prepared by use of different precursors

P. Jenuš[1], A. Iveković[1], M. Kocen[1,2], A. Šestan[2,3], S. Novak[1]

[1] Department for Nanostructured Materials, Jožef Stefan Institute, Ljubljana, Slovenia

[2] Jožef Stefan International Postgraduate School, Ljubljana, Slovenia

[3] Center for Electron Microscopy and Microanalysis, Jožef Stefan Institute, Ljubljana, Slovenia

Abstract

Tungsten is considered as a primary candidate material for high-heat-loaded structural parts in a demonstration fusion power plant, DEMO. Its recrystallisation at high temperatures, which results in a loss of strength, can be suppressed by incorporation of ceramic particles in the likes of oxides or carbides. Here we propose reinforcement of W-matrix with W_2C ceramic inclusions, which can be formed by high-temperature reaction of W-matrix with carbide precursor. In this study, W_2C particles are synthesised *in-situ* during vacuum sintering using three carbon sources: graphene, phenol-formaldehyde resin, and WC nanoparticles. Our results suggest that WC nanoparticles are the most suitable carbon source for the formation of W_2C-W composite. The composite containing 24 wt % of W_2C shows the denser structure and better mechanical properties compared to the pure tungsten. Additionally, ageing tests confirmed that incorporation of W_2C ceramic particles prevents the W-grain growth even at temperatures higher than 1200 °C.

Keywords: A sintering, B inclusions, C mechanical properties, E nuclear applications

1.1. Introduction

The development of advanced structural materials is one of the critical challenges for realising a commercially viable fusion power. Currently, no material solution has been confirmed as fully meeting the physical and system requirements for the demonstration fusion power plant (DEMO) and therefore, intensive collaborative research work is taking part in the EUROfusion programme.[1] For quite some time SiC-based ceramics were the subject of intensive studies[2–4] being a promising candidate for structural parts of future fusion reactors. Although the level of the development of SiC-based composites has increased remarkably, the fusion community decided that SiC-based ceramic composites were not yet sufficiently mature to be considered as viable and safe option for future

fusion power plants.[3] At the moment tungsten is considered as a primary candidate for high-heat-loaded structural parts in DEMO device, mainly due to its very high melting point, good thermal conductivity, and low sputtering yield.

Unfortunately, these advantages are accompanied by high-temperature recrystallisation, resulting in loss of strength.[5] Several approaches have been used to make tungsten tougher and less prone to loss of mechanical properties due to grain growth. The use of alloys (alloying of W with Ti, V, Ta, and Re) was proved inappropriate in the early stage of research.[5,6] For instance, W-Re alloy, exhibits advantageous ductile-to-brittle-transition temperature (DBTT) and recrystallisation temperature (RCT) and good mechanical properties, however, drawbacks in the application include its strongly reduced thermal conductivity and the formation of additional brittle phases due to the significant transmutation of W into Re.[6] One of the approaches investigated was also a combination of conventional powder metallurgy processing of tungsten followed by severe plastic deformation, i.e. rolling at low temperatures.[7,8] Such materials reflect increased mechanical properties at room temperature, but long-term exposure to high temperatures may result in recrystallisation and extensive grain growth.[9,10]

Recrystallisation of W can be limited by dispersion strengthening with oxide (Y_2O_3, La_2O_3)[11,12] or carbide (TiC, TaC)[13,14] ceramic nanoparticles in the W-matrix. Namely, these ceramic inclusions cause pinning of grain boundaries thus preventing the exaggerated grain growth of W during the recrystallisation. It was shown that the addition of oxide particles increases the recrystallisation temperature (for 100–350 K).[5] However, the addition of oxides with a melting temperature lower than the tungsten has an adverse effect on the erosion resistance.[5] While it was shown that the addition of TiC particles also improves the ductility with superplastic behaviour at temperatures 1400–1700 °C, the thermal stability of TiC precipitates when exposed to deuterium or He plasma at elevated temperatures is insufficient.[5,15] Increase in the recrystallisation temperature was also observed for the TaC reinforced W. However, due to the formation of secondary phases (i.e., TaO_2, mixed carbides) during the processing, the use of TaC as a candidate for reinforced W is less favourable.[15]

The aim of this study was to employ the concept of dispersion strengthening of W matrix with W_2C particles in order to prevent the W grain growth during its recrystallisation. This was achieved by reactive sintering of tungsten with different carbon precursors in a high-temperature vacuum furnace. Phase composition, morphology and mechanical properties of as-sintered samples were investigated. To examine the microstructure at elevated temperatures were as-sintered samples aged at 1250 °C for 24 h.

2.1. Experimental

W_2C inclusions were synthesised *in-situ* using three carbon sources: graphene (60 nm flakes, Grade AO-4, Graphene Supermarket, USA), phenol-formaldehyde resin (rezol, Fenolit, Slovenia), and WC nanoparticles (Tungsten(IV) carbide, nanopowder, 150-200 nm, >99%, Aldrich, Germany). Commercial tungsten powder (MPO7R, 99.9 %, Global Tungsten & Powder, ZDA) with submicron-sized particles (d_{50}= 0.7 µm) was mixed with a carbon source using the following procedure. Powder mixtures were homogenised in cyclohexane using the ultrasonic processor (UP400S – Hielscher Ultrasonic) for 3 min at 50 % strength and amplitude 1 s^{-1}. To preserve the obtained homogeneity after mixing, the suspension was freeze-dried using liquid nitrogen. The solvent was removed from the mixture by sublimation under reduced pressure. The powder mixture was then pressed into pellets with a diameter of 21 mm and height of approximately 2 mm using a uni-axial press (Paul-Otto Weber, Maschinen und Apparatebau, Germany) at 150 MPa followed by isostatic pressing (RP2000QC/LC, Recherches & Realisations Remy, France) at 800 MPa. Consolidation and *in-situ* formation of W_2C inclusions were carried out in a vacuum furnace (Astro, Thermal Technologies, USA), which was prior to the heating purged several times (3 or more) with argon, at 2200 °C for 6 h. Heating and cooling rate was 5 °/min. As-sintered pellets were, before phase and microstructural analysis and mechanical testing, ground and polished in order to remove a potentially contaminated top layer. The density of the composites was calculated from the pellets' dimensions.

X-ray powder diffraction (XRD- Bruker AXS Configuration utilising CuKα radiation at room temperature, the step width of 0.02°, fixed time of 1 s, a scanning range of 2θ: 20° to 80°) was used for the characterisation of phase composition of initial powder and sintered composites. The morphology of sintered samples was assessed by scanning electron microscopy (FE-SEM, JSM-7600F, Jeol Inc.). Analyses of diffraction data were performed with EVA and TOPAS software (Bruker AXS, Karlsruhe, Germany). The W_2C content was determined by Rietveld refinement of experimental XRD spectra. For the microstructural detection and identification of the secondary phase, energy-dispersive X-ray spectroscopy (EDS-X-max, Oxford Instruments equipped on FEI HeliosNanolab 650) and electron backscatter diffraction (EBSD-Channel 5, Oxford Instruments on FE-SEM), were performed. Simulations of EDS spectra were carried out with NIST DTSA II[16] software. Flexural strength test was done using Piston on three Balls technique (Galdabini Quasar 50, Italy). The hardness of the materials was measured with Vickers indentation test with the load of 500 N (Innovatest, Nexus 7500, Netherland). The grain size distribution sample was obtained from a

planimetric analysis conducted on four SEM micrographs per sample taking into account ≥ 500 grains using image-analysis software (ImageJ).

The samples with various compositions (up to 16.7 at % of added carbon) will be denoted as WxG, WxPF and WxWC, where *x* stands for the atomic fraction of added carbon and G for graphene, PF for phenol-formaldehyde resin and WC for WC nanoparticles (Table 1).

Table 1: Prepared mixtures of powders

sample **Addition of C**	W	W9G	W16G	W9PF	W16PF	W8WC	W16WC
at. %	0	8.6	16.7	8.6	16.7	7.2	16.7

3.1. Results and discussion

3.1.1 Phase composition

Figure 1a is showing diffraction patterns of pure W and composites of W with various carbon precursors and a final carbon concentration of 16.7 at %. In the sample prepared from a pure W, only peaks characteristic for cubic tungsten were observed, while in all the samples with added C-precursor, trigonal W_2C peaks were also identified.

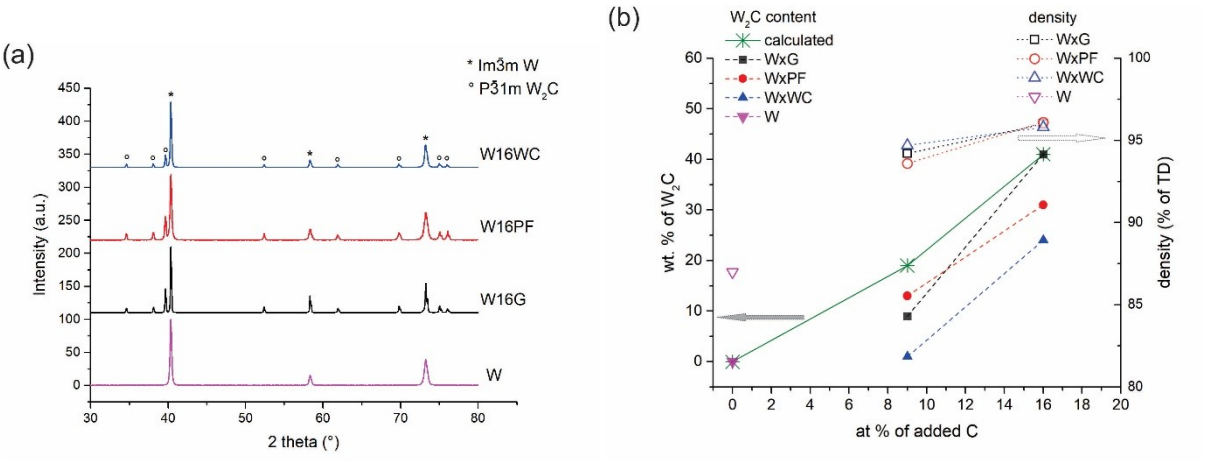

Figure 1: (a) XRD diffractograms of pure W and W_2C-W composites with 16.7 at % of added carbon in the form of various precursors, and (b) wt % of the W_2C phase and relative densities in the sintered samples depending on the amount of added carbon and type of precursor.

The results of the Rietveld analysis presented in Figure 1b suggest that regardless of the type of precursor used, the amount of W_2C synthesised *in-situ* during the reactive sintering increases with an increase in the starting concentration of carbon. However, the measured amounts of W_2C were lower from the expected (calculated), which implies that either a part of carbon precursor remained unreacted or a part of carbon was consumed for the reduction of the oxide residues present in the starting powder. The second explanation seems to be more probable as no remains of the added

precursors were observed in the microstructure of sintered samples (Figure 2) or were detected by XRD analysis (Figure 1). As evident, the content of the formed W_2C phase differs for the same amount of added C-precursor with selected precursors. The highest W_2C contents were observed for the samples WxG in which 8.6 or 16.7 at. % of carbon was added in the form of graphene. None of the samples revealed the presence of unreacted graphene. On the other hand, the lowest content of W_2C was identified in the composites prepared from WC ceramic nanoparticles as a carbon source. The composition of the W8WC composite could not be accurately determined by Rietveld analysis because the amount of formed W_2C phase was below the detection limit of laboratory XRD. Although the determined amount of W_2C was much lower than expected (25 wt. % instead of 41 wt. % for W16WC sample), no remaining WC was detected by XRD analysis. A possible explanation for the discrepancy between the calculated and determined amount of W_2C is that a part of carbon from the precursor is used for the reaction with present oxide.[17]

3.1.2. Microstructure

From the SEM micrographs presented in Figures 2 a-d the variation of the grain size and the porosity of the sintered samples as a result of different carbon precursors in tungsten matrix can be clearly observed. It can be seen that pure tungsten sintered in vacuum at 2200 °C for 6 h (Fig. 2a) is highly porous, which is in agreement with the measured density (Fig. 1b). In pure W, besides the observed intragranular porosity, the pores are present at the grain boundaries as well. As expected, the *in situ* formation of W_2C ceramic inclusions in W matrix resulted in smaller average grain size of W, as well as in the decrease in porosity. From Figures 2 b – d it can be seen that the intragranular porosity of composites is strongly reduced. This feature can also be seen from the fractured surfaces (insets of Fig 2). The morphology of fractured surfaces (insets in Fig.2) is similar in all investigated materials. Namely, the fractured surfaces display typical brittle behaviour with a combination of intergranular fracture of smaller grains and inclusions with the transgranular fracture of larger W grains. It looks like the addition of ceramic particles in the W-matrix does not strengthen the grain boundaries. However, it obviously deflects the crack propagation path as a result of higher measured hardness of ceramic W_2C inclusions when compared to pure W, leading to an increase in mechanical properties.

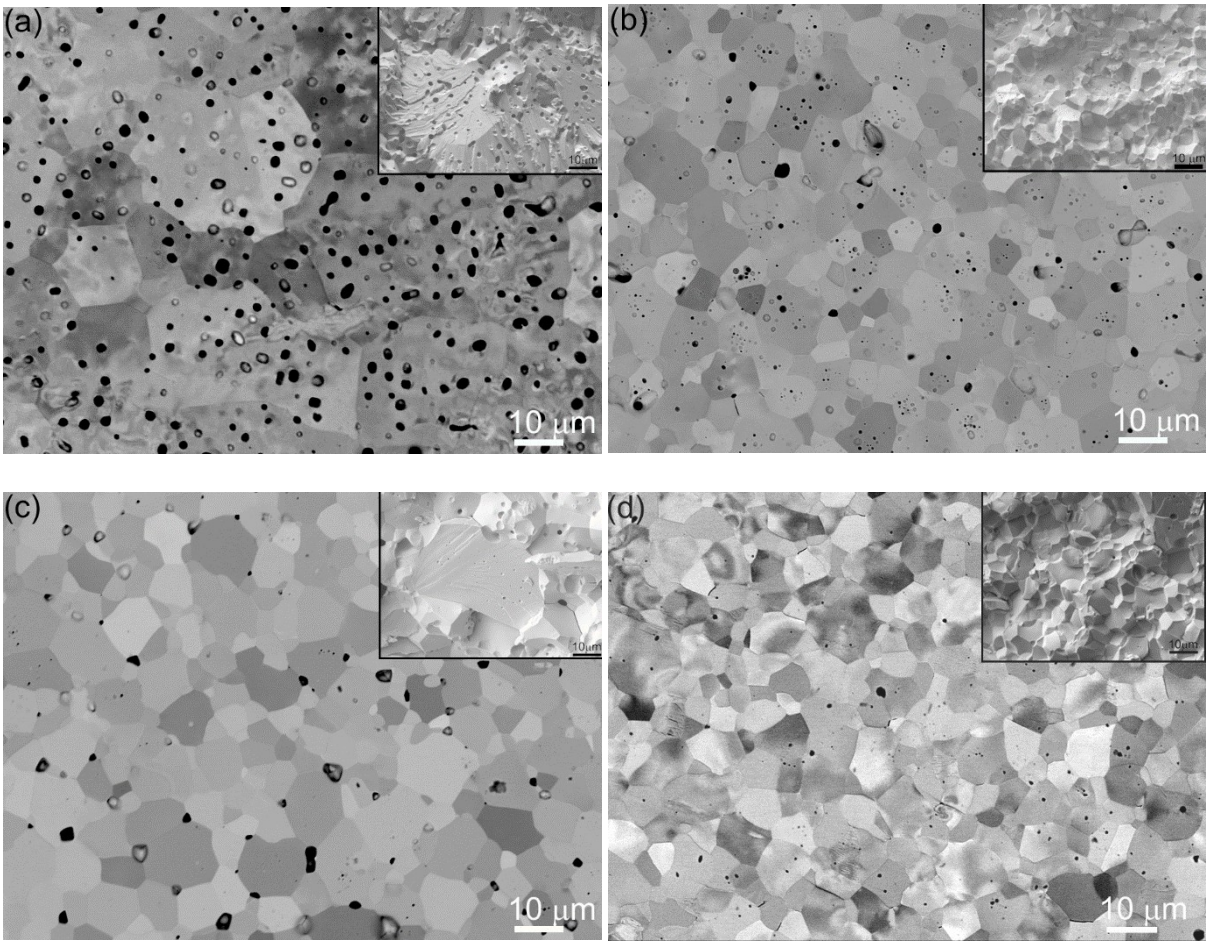

Figure 2: SEM micrographs were taken with backscattered electrons on polished surfaces of (a) pure W, and W_2C-W composites with 16.7 at % of carbon added in the form of various precursors: b) graphene, c) phenol-formaldehyde resin, d) WC nanoparticles. Inset images represent fractured surfaces of the corresponding samples.

The presence of W_2C inclusions in W matrix cannot be identified by observation in a backscattered electron mode (BEI) in SEM due to the channelling of electrons in W grains, caused by random/different orientation, which is being observed as different contrast (Fig. 2). Furthermore, the energy dispersive X-ray spectroscopy (EDS) cannot provide reliable results about elemental composition in W_2C-W composites due to the overlapping of W N-lines (N4 255.9 eV, N5 243.5 eV) with C K-line (298.2 eV). Therefore, the energy backscatter diffraction (EBSD) was used to identify W_2C (P-31m) inclusions within W matrix (Im-3m). Figure 3 represents the EBSD pattern of the W16WC sample. It can be seen that W_2C grains (in red), with sizes smaller than the W ones (in blue), are distributed at W grain boundaries. Such distribution is indicative of pinning of W grain boundaries, thus preventing W grain growth and/or pore entrapment in the grains.

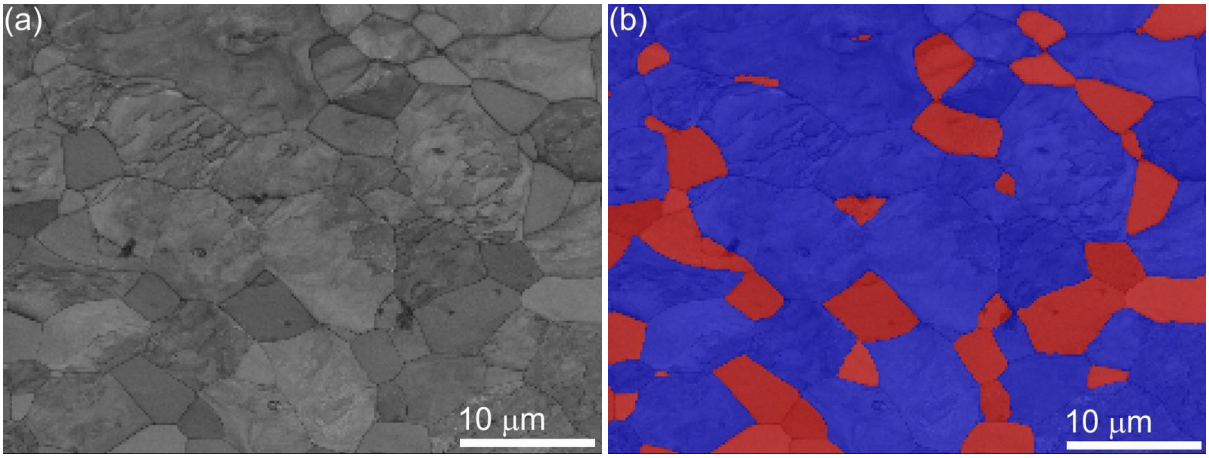

Figure 3: SEM images of W16WC sample: (a) secondary electrons image and (b) EBSD phase distribution in which red represents P-31m W_2C and blue represent Im-3m W.

3.1.3. Mechanical properties

Flexural strength and Vickers hardness of the sintered samples are presented in Figure 4. Figure 4a reveals that despite significantly reduced porosity achieved by the addition of carbon, the flexural strength is only increased for samples with addition of WC ceramic nanoparticles, while the addition of graphene and phenol formaldehyde resin resulted in a decrease of the flexural strength when compared to pure tungsten samples sintered under the same conditions. The variance in the flexural strength with the carbon precursor can be most likely ascribed to the different chemical reaction during *in-situ* formation of W_2C phase: while carbon from graphene and phenol formaldehyde resin reacts with the surrounding tungsten grains, the WC loses a part of carbon due to the gradient-enhanced diffusion to form W_2C [18]. Furthermore, as an organic source of carbon, phenol formaldehyde resin has to undergo the process of the pyrolysis before only carbon remains. It is known that during the pyrolysis of phenol formaldehyde resin several volatile species are formed [19], which can be the reason for the formation of larger voids/pores in the WxPF composites, a potentially critical strength-limiting flaws leading to a decrease in mechanical properties of the composite. The highest flexural strength was achieved for the sample with 7.2 at % of added C in the form of WC nanoparticles (sample W8WC), which contains only small amount (< 3 wt %) of W_2C phase. Figure 4b presents the dependence of composites hardness for the samples containing different amount of W_2C phase. As expected due to the much higher Vickers hardness of W_2C than W (19 GPa and 3.43 GPa, respectively), an increase in HV with increasing W_2C content can be observed. With 16.7 at % of added carbon, the highest hardness (6.5 GPa) was displayed by the sample in which graphene (W16G) was used as a carbon precursor and which had the highest content of W_2C phase (41 wt %). When taking into account both quantities, namely flexural strength and hardness, the

samples, in which WC was used as a carbon precursor for the formation of W_2C inclusions, display the most promising properties.

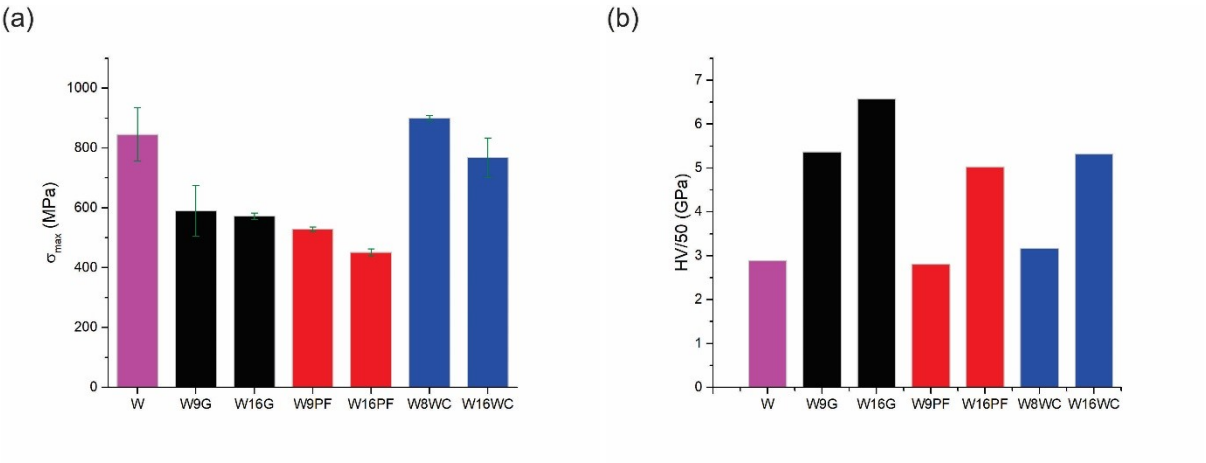

Figure 4: Flexural strength (a) and Vickers hardness (b) of sintered samples.

3.1.4. Ageing

One of the disadvantages of tungsten is its recrystallisation at temperatures higher than 1000 °C, as expected in the DEMO divertor.[5] At those temperatures exaggerated growth of W grains also occurs, which results in the deterioration of mechanical properties. Stabilising the microstructure with the *in situ* formation of ceramic inclusions was supposed to prevent or at least minimise W grain growth and thus preserve its mechanical properties[5]. To examine the evolution of microstructure at high temperatures, the sintered samples were aged in a vacuum furnace at 1250 °C for 24 h. Polished surfaces of pure W and W16WC samples after ageing are presented in Figure 5a and 5b, respectively. The microstructural analysis confirmed that ceramic W_2C inclusions dispersed in W-matrix (Fig. 5b) substantially suppress the growth of W grains. When comparing the as-sintered (Fig. 2) and aged (Fig. 5) samples the difference in the grain size of pure W and W_2C-reinforced W after ageing is even more pronounced. While there is no grain growth in the composite, the size of W grains in pure W increases significantly. Grain size analysis of aged samples (Fig. 5c) revealed that the average grain size for the pure tungsten is 11.8 μm, while in the W16WC it is 5.8 μm. Moreover, the W16WC sample is displaying very narrow monomodal grain size distribution, whereas the distribution of pure tungsten is pointing towards a bimodal grain size distribution, with fractions of larger grains in size range of 15–25 μm indicating exaggerated grain growth. The suppression of growth of W grains was the case in all investigated W_2C-reinforced W samples regardless of the type of C-precursor used for the formation of ceramic W_2C phase.

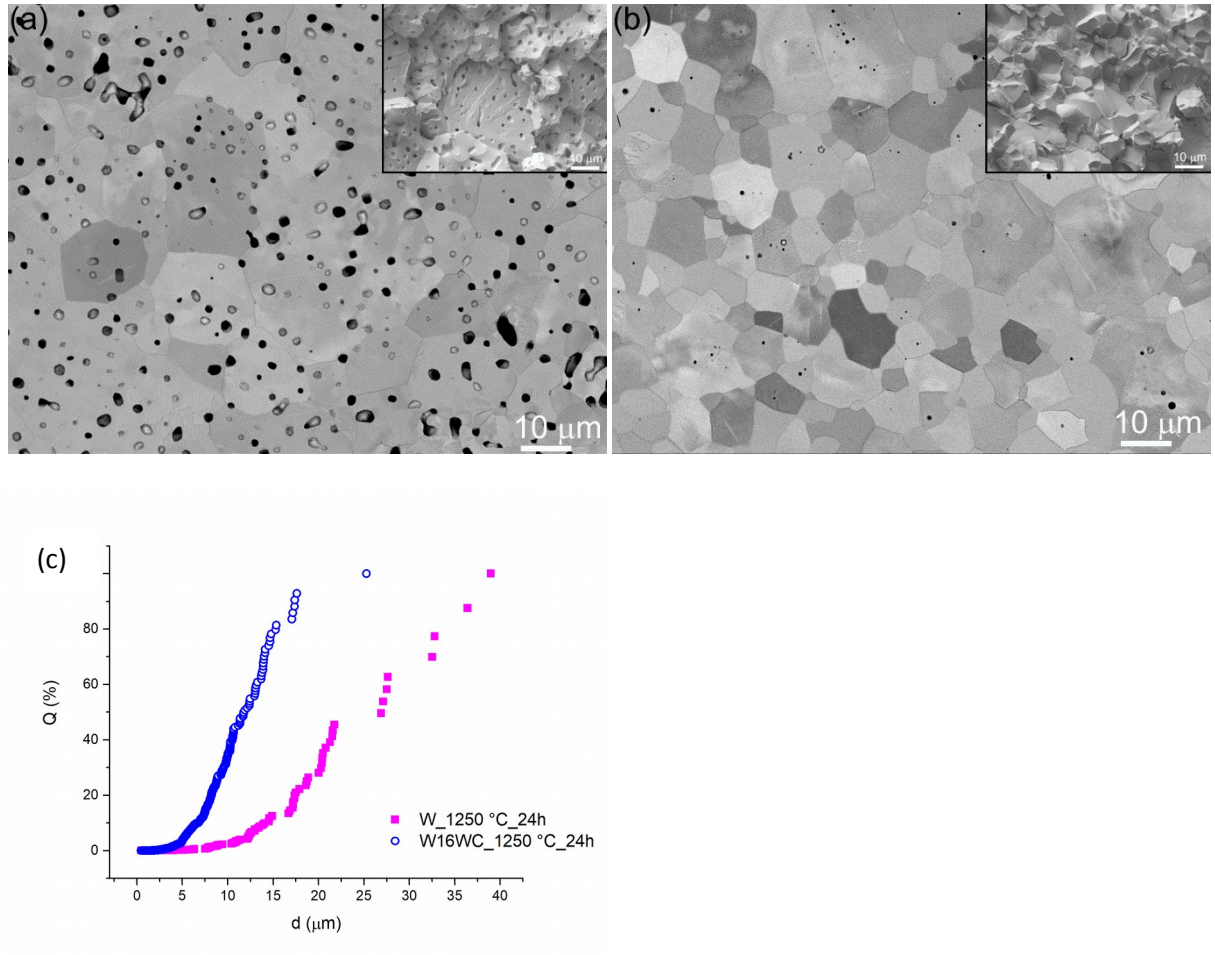

Figure 5: SEM-BEI micrographs of the polished surface of W (a) and W16WC (b) sample after ageing at 1250 °C for 24 h. Fractured surfaces of the same samples in the inset. (c) Grain size distribution for samples W and W16WC after ageing.

4.1. Conclusions

The matrix of metallic tungsten was successfully reinforced by *in-situ* formed W_2C ceramic inclusions that eliminated intra- and inter-granular porosity and substantially refined the microstructure. W_2C formation during sintering was provoked by using three carbon precursors: graphene, phenol-formaldehyde resin, and WC nanoparticles. Phase analysis of the samples sintered in a vacuum furnace at 2200 °C for 6 hours confirmed the presence of only two phases, W_2C and W, respectively. Moreover, the newly formed carbide grains successfully inhibited W grain growth also after prolonged ageing at 1250 °C for 24 h. Significantly reduced porosity and refined microstructures resulted in improvement of mechanical properties for the WxWC composite, containing small amounts (< 3 to 24 wt %) of W_2C ceramic phase in W-matrix when compared to the pure W prepared under the same conditions. The presented approach of *in-situ* formation of W_2C ceramic inclusions within the host matrix can be used not only for the preparation of W_2C-W composites for nuclear fusion applications but also for other high-temperature applications.

Acknowledgement:

This work has been carried out within the framework of the EUROfusion Consortium and has received funding from the Euratom research and training programme 2014-2018 under grant agreement No 633053. The views and opinions expressed herein do not necessarily reflect those of the European Commission. Financial support from the Slovenian Research Agency (research core funding No. P2-0087) is acknowledged. Parts of the work have been performed within the PhD studies of Ms Andreja Šestan and Mr Matej Kocen; both supported by the EUROfusion education & training scheme. Authors would also like to thank to Assist Prof Dr Andraž Kocjan for fruitful discussions.

References

1. EUROfusion. Available at: https://www.euro-fusion.org/.
2. Hinoki, T. *et al.* Silicon Carbide and Silicon Carbide Composites for Fusion Reactor Application. *Mater. Trans.* **54,** 472–476 (2013).
3. Iveković, A., Novak, S., Dražić, G., Blagoeva, D. & de Vicente, S. G. Current status and prospects of SiCf/SiC for fusion structural applications. *J. Eur. Ceram. Soc.* **33,** 1577–1589 (2013).
4. Riccardi, B. *et al.* Issues and advances in SiCf/SiC composites development for fusion reactors. *J. Nucl. Mater.* **329–333,** 56–65 (2004).
5. Pintsuk, G. *Tungsten as a plasma-facing material*. *Comprehensive Nuclear Materials* **4,** (Elsevier Inc., 2012).
6. Norajitra, P. *Divertor development for a future fusion power plant*. *Journal of Chemical Information and Modeling* **53,** (2013).
7. Wei, Q. & Kecskes, L. J. Effect of low-temperature rolling on the tensile behavior of commercially pure tungsten. *Mater. Sci. Eng. A* **491,** 62–69 (2008).
8. Wei, Q., Kecskes, L. J. & Ramesh, K. T. Effect of low-temperature rolling on the propensity to adiabatic shear banding of commercial purity tungsten. *Mater. Sci. Eng. A* **578,** 394–401 (2013).
9. Wei, Q. *et al.* Microstructure and mechanical properties of super-strong nanocrystalline tungsten processed by high-pressure torsion. *Acta Mater.* **54,** 4079–4089 (2006).
10. Rieth, M. *et al.* Recent progress in research on tungsten materials for nuclear fusion applications in Europe. *J. Nucl. Mater.* **432,** 482–500 (2013).
11. Liu, R. *et al. Microwave synthesis and properties of fine-grained oxides dispersion strengthened tungsten*. *Journal of Nuclear Materials* **424,** (2012).
12. Kim, Y., Lee, K. H., Kim, E.-P., Cheong, D.-I. & Hong, S. H. Fabrication of high temperature oxides dispersion strengthened tungsten composites by spark plasma sintering process. *Int. J. Refract. Met. Hard Mater.* **27,** 842–846 (2009).
13. Kitsunai, Y. *et al.* Microstructure and impact properties of ultra-fine grained tungsten alloys dispersed with TiC. *J. Nucl. Mater.* **271,** 423–428 (1999).
14. Lang, S. *et al.* Microstructure, basic thermal–mechanical and Charpy impact properties of W-0.1 wt.% TiC alloy via chemical method. *J. Alloys Compd.* **660,** 184–192 (2016).

15. Kurishita, H. *et al.* Current status of nanostructured tungsten-based materials development. *Phys. Scr.* **T159,** 14032 (2014).

16. Small, J. A. *et al.* Modeling of the bremsstrahlung radiation produced in pure-element targets by 10–40 keV electrons. *J. Appl. Phys.* **61,** 459–469 (1987).

17. Šestan, A., Jenuš, P., Krmpotič, S. N., Zavašnik, J. & Čeh, M. The role of tungsten phases formation during tungsten metal powder consolidation by FAST: Implications for high-temperature applications. *Mater. Charact.* (2018). doi:10.1016/j.matchar.2018.02.022

18. Suetin, D. V., Shein, I. R., Kurlov, a. S., Gusev, a. I. & Ivanovskiĭ, a. L. Band structure and properties of polymorphic modifications of lower tungsten carbide W2C. *Phys. Solid State* **50,** 1420–1426 (2008).

19. Jiang, H. *et al.* The pyrolysis mechanism of phenol formaldehyde resin. *Polym. Degrad. Stab.* **97,** 1527–1533 (2012).